Joint 9D Receiver Localization and Ephemeris Correction with LEO and 5G Base Stations

Don-Roberts Emenonye, Harpreet S. Dhillon, and R. Michael Buehrer

Abstract-In this paper, we use the Fisher information matrix (FIM) to analyze the interaction between low-earth orbit (LEO) satellites and 5G base stations in providing 9D receiver localization and correcting LEO ephemeris. First, we give a channel model that captures all the information in the LEOreceiver, LEO-BS, and BS-receiver links. Subsequently, we use FIM to capture the amount of information about the channel parameters in these links. Then, we transform these FIM for channel parameters to the FIM for the 9D (3D position, 3D orientation, and 3D velocity estimation) receiver localization parameters and the LEO position and velocity offset. Closedform expressions for the entries in the FIM for these location parameters are presented. Our results on identifiability utilizing the FIM for the location parameters indicate: i) with one LEO, we need three BSs and three time slots to both estimate the 9D location parameters and correct the LEO position and velocity, ii) with two LEO, we need three BSs and three time slots to both estimate the 9D location parameters and correct the LEO position and velocity, and iii) with three LEO, we need three BSs and fourtime slots to both estimate the 9D location parameters and correct the LEO position and velocity. We notice from the Cramer Rao lower bound that the operating frequency and number of receive antennas have negligible impact on the estimation accuracy of the orientation of the receiver and the LEO velocity, respectively.

Index Terms—6G, LEO, 9D localization, FIM, 3D position, 3D velocity, and 3D orientation, theoretical LEO ephemeris correction.

I. INTRODUCTION

The challenge of providing quality global connectivity has led to the deployment of satellites in existing low-earth orbit (LEO) constellations and the creation of new constellations. This can be seen in older constellations Orbcomm, Iridium, and Globalstar, as well as in newly created constellations such as Boeing, SpaceMobile, OneWeb, Telesat, Kuiper, and Starlink. Since these constellations will be closer to the earth than the medium earth orbit (MEO) satellites, they will encounter a shorter propagation time and lower propagation losses than the current Global Navigation Satellite System (GNSS); their utility for positioning is an area of natural interest. Moreover, these LEOs could be used as a backup during the inevitable scenarios where GNSS becomes unavailable, such as in deep urban canyons, under dense foliage, during unintentional interference, and intentional jamming) or untrustworthy (e.g., under malicious spoofing attacks). Because of these reasons,

D.-R. Emenonye, H. S. Dhillon, and R. M. Buehrer are with Wireless@VT, Bradley Department of Electrical and Computer Engineering, Virginia Tech, Blacksburg, VA, 24061, USA. Email: {donroberts, hdhillon, rbuehrer}@vt.edu. The support of the US National Science Foundation (Grants ECCS-2030215, CNS-1923807, and CNS-2107276) is gratefully acknowledged.

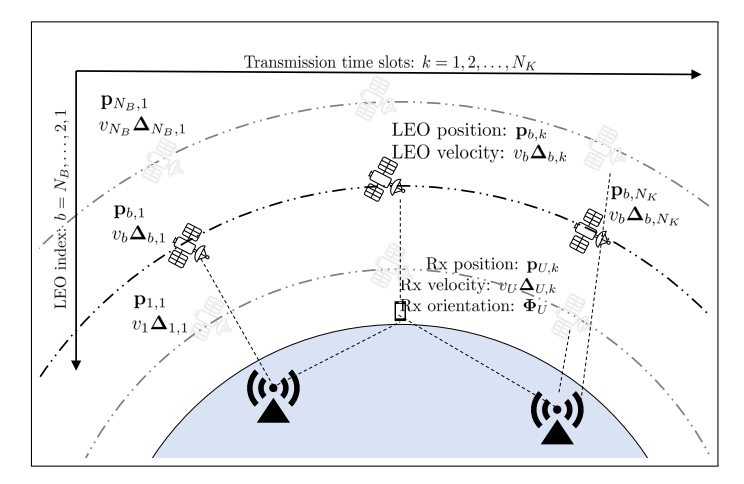


Figure 1. Joint 9D Receiver Localization and Ephemeris Correction with N_B LEO and N_Q 5G Base Stations transmitting during N_K transmission time slots to a receiver with N_U antennas.

there has been a surge in research on the utility of LEOs for localization.

A. Prior Art

In [1], [2], a Fisher information matrix (FIM) based rigorous investigation of the utility of LEOs for 9D localization is presented where it is shown that obtaining delay and Doppler measurements from three satellites over three times slots over multiple receive antenna enables 9D localization. In [3], the signal structure is assumed to be known, and delay measurements are used to localize a receiver. The authors in [4] investigate using satellites deployed to provide broadband internet connectivity to assist localization. The proposed framework will use delay measurements and describe the positioning errors as a function of the geometric dilution of precision (GDOP) to provide a benchmark. In [5], Doppler measurements obtained from Amazon Kuiper Satellites are used for receiver positioning. In [6], LEOs meet integrated sensing and localization, and the positioning information obtained from the LEOs is used to improve the transmission rate. The authors in [7] utilize eight Doppler measurements to estimate the 3D position, 3D velocity, clock rate, and clock offset. In [8], an opportunistic experimental framework is developed to estimate position, clock, and correct LEO ephemeris. An unmanned aerial vehicle (UAV) is tracked for two minutes using the received signals from two Orbcomm satellites in [9].

Although, there has been some work on using LEOs for localization, the current state of the art has failed to rigorously characterize the interplay between the information from the

LEOs and 5G base station (BSs) for both 9D localization and LEO ephemeris correction. Hence, in this paper, we utilize the FIM to rigorously present the available information that is obtainable in the LEO-receiver link, LEO-BS link, and BS-receiver and the utility of this information for joint 9D receiver localization and LEO ephemeris correction, which leads to critical insights on the interplay between number of LEOs, BSs, operating frequency, number of transmission time slots, the combination of synchronized BSs and unsynchronized LEOs, and the number of receive antennas.

Notation: The function $F_{\boldsymbol{v}}(\boldsymbol{w}; \boldsymbol{x}, \boldsymbol{y}) \triangleq \mathbb{E}_{\boldsymbol{v}} \left\{ \left[\nabla_{\boldsymbol{x}} \ln f(\boldsymbol{w}) \right] \left[\nabla_{\boldsymbol{y}} \ln f(\boldsymbol{w}) \right]^{\mathrm{T}} \right\}$ and $G_{\boldsymbol{v}}(\boldsymbol{w}; \boldsymbol{x}, \boldsymbol{y})$ describes the loss of information in the FIM defined by $F_{\boldsymbol{v}}(\boldsymbol{w}; \boldsymbol{x}, \boldsymbol{y})$ due to uncertainty in the nuisance parameters. The inner product of \boldsymbol{x} is $\|\boldsymbol{x}\|^2$ and the outer product of \boldsymbol{x} is $\|\boldsymbol{x}^{\mathrm{T}}\|^2$. $\nabla_{\boldsymbol{x}} \boldsymbol{y}$ is the first derivative of \boldsymbol{y} with respect to \boldsymbol{x} .

II. SYSTEM MODEL

We consider N_B single antenna LEO satellites, N_O single antenna BSs, and a receiver with N_U antennas. The N_B LEOs communicate with the N_Q BSs and the receiver over N_K transmission time slots as shown in Fig. 1. Similarly, the N_Q BSs communicate over N_K transmission time slots with the receiver. There is a Δ_t spacing between the N_K transmission slots. The LEOs are located at $p_{b,k}$ $\{1, 2, \cdots, N_B\}$ and $k \in \{1, 2, \cdots, N_K\}$ while the BSs are located at $p_{q,k} \ q \in \{1, 2, \dots, N_Q\}$ and $k \in \{1, 2, \dots, N_K\}$. Finally, the receiver is located at $p_{U,k}$ $k \in \{1, 2, \dots, N_K\}$. The LEOs, BSs, and receiver positions are defined with respect to a global origin and a global reference axis. The position of the antennas on the receiver can be defined with respect to the receiver's centroid as $s_u = Q_U \tilde{s}_u$ where \tilde{s}_u aligns with the global reference axis and $Q_U = Q(\alpha_U, \psi_U, \varphi_U)$ defines a 3D rotation matrix [10]. The orientation angles of the receiver are vectorized as $\mathbf{\Phi}_U = \left[\alpha_U, \psi_U, \varphi_U\right]^{\mathrm{T}}$. The point, s_u can be described with respect to the global origin as $p_{u,k} = p_{U,k} + s_u$. The receiver's centroid can be described with respect to the position of the b^{th} LEO satellite as $\boldsymbol{p}_{U,k} = \boldsymbol{p}_{b,k} + d_{bU,k} \boldsymbol{\Delta}_{bU,k}$ where $d_{bU,k}$ is the distance from point $p_{b,k}$ to point $p_{U,k}$ and $\Delta_{bU,k}$ is the corresponding unit direction vector $\Delta_{bU,k} = [\cos \phi_{bU,k} \sin \theta_{bU,k}, \sin \phi_{bU,k} \sin \theta_{bU,k}, \cos \theta_{bU,k}]^{\mathrm{T}}.$ The receiver's u^{th} antenna can be described with respect to the position of the b^{th} LEO satellite as $oldsymbol{p}_{u,k} = oldsymbol{p}_{b,k}$ + $d_{bu,k}\Delta_{bu,k}$ where $d_{bu,k}$ is the distance from point $p_{b,k}$ to point $p_{u,k}$ and $\Delta_{bu,k}$ is the corresponding unit direction vector $\Delta_{bu,k} = [\cos \phi_{bu,k} \sin \theta_{bu,k}, \sin \phi_{bu,k} \sin \theta_{bu,k}, \cos \theta_{bu,k}]^{\mathrm{T}}.$ The receiver's centroid can be described with respect to the position of the q^{th} BS as $p_{U,k} = p_{q,k} + d_{qU,k} \Delta_{qU,k}$ where $d_{qU,k}$ is the distance from point $p_{q,k}$ to point $p_{U,k}$ and $\Delta_{qU,k}$ is the corresponding unit direction vector $\Delta_{qU,k} = [\cos \phi_{qU,k} \sin \theta_{qU,k}, \sin \phi_{qU,k} \sin \theta_{qU,k}, \cos \theta_{qU,k}]^{\mathrm{T}}.$ The receiver's u^{th} antenna can be described with respect to the position of the q^{th} BS as $\boldsymbol{p}_{u,k} = \boldsymbol{p}_{q,k} + d_{qu,k} \boldsymbol{\Delta}_{qu,k}$ where $d_{qu,k}$ is the distance from point $p_{q,k}$ to point $oldsymbol{p}_{u,k}$ and $oldsymbol{\Delta}_{qu,k}$ is the corresponding unit direction vector $\Delta_{qu,k} = [\cos \phi_{qu,k} \sin \theta_{qu,k}, \sin \phi_{qu,k} \sin \theta_{qu,k}, \cos \theta_{qu,k}]^{\mathrm{T}}.$ The qth BS can be described with respect to the position of the b^{th} LEO as $\boldsymbol{p}_{q,k} = \boldsymbol{p}_{b,k} + d_{bq,k} \boldsymbol{\Delta}_{bq,k}$ where $d_{bq,k}$ is the distance from point $\boldsymbol{p}_{b,k}$ to point $\boldsymbol{p}_{q,k}$ and $\boldsymbol{\Delta}_{bq,k}$ is the corresponding unit direction vector $\boldsymbol{\Delta}_{bq,k} = [\cos \phi_{bq,k} \sin \theta_{bq,k}, \sin \phi_{bq,k} \sin \theta_{bq,k}, \cos \theta_{bq,k}]^{\mathrm{T}}$.

A. Transmit and Receive Processing

There are three transmission scenarios to consider: i) LEO-receiver link, ii) LEO-BS link, and iii) BS-receiver link. At time t, during $k^{\rm th}$ transmission time slot, the N_B LEOs communicate with the N_Q BSs and receiver over N_K transmission time slots using quadrature modulation. The $b^{\rm th}$ LEO transmits the following symbol

$$x_{b,k}[t] = s_{b,k}[t] \exp(j2\pi f_c t),$$
 (1)

where $s_{b,k}[t]$ is the modulation symbol and $f_c = \frac{c}{\lambda}$ is the operating frequency. Here, c is the speed of light, and λ is the wavelength. In this work, in the LEO-receiver link, only the line of sight paths are considered, and the useful part of the signal received at time t, during k^{th} transmission time slot on the u^{th} receive antenna is

$$\mu_{bu,k}[t] = \beta_{bu,k} \sqrt{2} \Re \left\{ s_{b,k}[t_{obu,k}] \exp(j(2\pi f_{obU,k} t_{obu,k})) \right\}.$$
(2)

Here, $\beta_{bu,k}$ is the channel gain at the u^{th} receive antenna during the k^{th} time slot. The effective time duration from the b^{th} LEO to the u^{th} receive antenna is $t_{obu,k} = t - \tau_{bu,k} + \delta_{bU}$ and the effective frequency observed at the receiver from the b^{th} LEO is $f_{obU,k} = f_c(1 - \nu_{bU,k}) + \epsilon_{bU}$. During the k^{th} time slot, the delay from the b^{th} LEO to the u^{th} receive antenna is $\tau_{bu,k} \triangleq \frac{\|\ddot{\mathbf{p}}_{u,k} - (\mathbf{p}_{b,k} + \check{\mathbf{p}}_{b,k})\|}{c}$. The time offset and frequency offset of the b^{th} LEO satellite with respect to the receiver is δ_{bU} and ϵ_{bU} , respectively. The point, $\check{\mathbf{p}}_{b,k}$ describes the uncertainty associated with the position of the bth LEO during the kth time slot. The Doppler observed at the receiver with respect to the b^{th} LEO satellite is $\nu_{bU,k} = \boldsymbol{\Delta}_{bU,k}^{\text{T}} \frac{(\boldsymbol{v}_{b,k} + \tilde{\boldsymbol{v}}_{b,k} - \boldsymbol{v}_{U,k})}{c}$. Here, $\boldsymbol{v}_{b,k} = v_b \boldsymbol{\Delta}_{b,k}$ and $v_{U,k} = v_U \Delta_{U,k}$ are the velocities of the b^{th} LEO and receiver, respectively. The speeds of the b^{th} LEO satellite and receiver are v_b and v_U , respectively. The associated directions are defined as $\Delta_{b,k} = [\cos \phi_{b,k} \sin \theta_{b,k}, \sin \phi_{b,k} \sin \theta_{b,k}, \cos \theta_{b,k}]^{\mathrm{T}}$ and $\Delta_{U,k} = [\cos \phi_{U,k} \sin \theta_{U,k}, \sin \phi_{U,k} \sin \theta_{U,k}, \cos \theta_{U,k}]^{\mathrm{T}}$, respectively. Here, $\check{\boldsymbol{v}}_{b,k}$ is the uncertainty related to the velocity of the b^{th} LEO during the k^{th} time slot.

In the LEO-BS link, only the line of sight paths are considered, and the useful part of the signal received at time t, during $k^{\rm th}$ transmission time slot on the $q^{\rm th}$ BS is

$$\mu_{bq,k}[t] = \beta_{bq,k} \sqrt{2} \Re \left\{ s_{b,k}[t_{obq,k}] \exp(j(2\pi f_{obq,k} t_{obq,k})) \right\}.$$
(3)

Here, $\beta_{bq,k}$ is the channel gain at the q^{th} BS during the k^{th} time slot. The effective time duration from the b^{th} LEO to the q^{th} BS is $t_{obq,k} = t - \tau_{bq,k} + \delta_{bQ}$ and the effective frequency observed at the q^{th} BS from the b^{th} LEO is $f_{obq,k} = f_c(1 - \nu_{bq,k}) + \epsilon_{bQ}$. During the k^{th} time slot, the delay from the b^{th} LEO to the q^{th} BS is $\tau_{bq,k} \triangleq \frac{\|\mathbf{p}_{q,k} - (\mathbf{p}_{b,k} + \check{\mathbf{p}}_{b,k})\|}{c}$. The time offset and frequency offset of the b^{th} LEO satellite with respect to the q^{th} BS is δ_{bQ} and ϵ_{bQ} , respectively. The Doppler observed at

the q^{th} BS with respect to the b^{th} LEO satellite is $\nu_{bq,k}=$

In the BS-receiver link, only the line of sight paths are considered, and the useful part of the signal received at time t, during k^{th} transmission time slot at the receiver is

$$\mu_{qu,k}[t] = \beta_{qu,k} \sqrt{2} \Re \left\{ s_{q,k}[t_{oqu,k}] \exp(j(2\pi f_{oqU,k} t_{oqu,k})) \right\}. \tag{4}$$

Here, $\beta_{qu,k}$ is the channel gain at the u^{th} antenna on the receiver from the q^{th} BS during the k^{th} time slot. The effective time duration from the q^{th} BS to the u^{th} antenna on the receiver is $t_{oqu,k} = t - au_{qu,k} + \delta_{QU}$ and the effective frequency observed at the u^{th} receive antenna from the q^{th} BS is $f_{oqU,k} = f_c(1 - \nu_{qU,k}) + \epsilon_{QU}$. During the k^{th} time slot, the delay from the q^{th} BS to the u^{th} receive antenna is $\tau_{qu,k} \triangleq \frac{\|\mathbf{p}_{u,k} - \mathbf{p}_{q,k}\|}{c}$. The time offset and frequency offset of BSs with respect to the receiver are δ_{QU} and ϵ_{QU} , respectively. The Doppler observed at the receiver with respect to the $q^{\rm th}$ BS is $\nu_{qU,k} = \Delta_{qU,k}^{\rm T} \frac{(0-v_{U,k})}{c}$. With this formulation, the received signal at the $u^{\rm th}$ receive antenna during the k^{th} time slot from the LEOs and BSs is

$$y_{1u,k}[t] = \sum_{q}^{N_Q} y_{qu,k}[t] = \sum_{q}^{N_Q} \mu_{qu,k}[t] + n_{u,k}[t],$$

$$y_{2u,k}[t] = \sum_{b}^{N_B} y_{bu,k}[t] = \sum_{b}^{N_B} \mu_{bu,k}[t] + n_{u,k}[t],$$
(5)

where $n_{u,k}[t] \sim \mathcal{CN}(0, N_{01})$ is the Fourier transformed thermal noise local to the receiver's antenna array. The received signal at the q^{th} BS during the k^{th} time slot from the LEOs is

$$y_{q,k}[t] = \sum_{k=1}^{N_B} y_{bq,k}[t] = \sum_{k=1}^{N_B} \mu_{bq,k}[t] + n_{q,k}[t],$$
 (6)

where $n_{q,k}[t] \sim \mathcal{CN}(0, N_{02})$ is the Fourier transformed thermal noise local to the q^{th} BS.

Remark 1. The offset δ_{bU} captures the unknown ionospheric and tropospheric delay concerning the bth LEO satellite as well as the time offset in the LEO-receiver link. Similarly, the offset δ_{bQ} captures the unknown ionospheric and tropospheric delay concerning the bth LEO satellite as well as the time offset in the LEO-BS link.

Here, the position of the b^{th} LEO satellite and the u^{th} receive antenna during the k^{th} time slot is $\mathbf{p}_{b,k} = \mathbf{p}_{b,o} + \tilde{\mathbf{p}}_{b,k}, \mathbf{p}_{u,k} = \mathbf{p}_{u,o} + \tilde{\mathbf{p}}_{U,k}$, where $\mathbf{p}_{b,o}$ and $\mathbf{p}_{u,o}$ are the reference points of the b^{th} LEO satellite and the u^{th} receive antenna, respectively. The distance travelled by the b^{th} LEO satellite and the u^{th} receive antenna are $\tilde{\mathbf{p}}_{b,k}$ and $\tilde{\mathbf{p}}_{u,k}$, respectively. These traveled distances can be described as $\tilde{\mathbf{p}}_{b,k} = (k-1)\Delta_t v_b \boldsymbol{\Delta}_{b,k}, \tilde{\mathbf{p}}_{U,k} = (k-1)\Delta_t v_U \boldsymbol{\Delta}_{U,k}$.

B. Received Signal Properties

The properties of the signal received across all N_K antennas from the N_B LEOs are described with the aid of the: i) Fourier transform of the baseband signal (spectral density) that is transmitted by the b^{th} LEO satellite at time t during the k^{th} time slot, $S_{b,k}[f] \triangleq \frac{1}{\sqrt{2\pi}} \int_{-\infty}^{\infty} s_{b,k}[t] \exp(-j2\pi ft) dt$, and ii) Fourier transform of the baseband signal (spectral density) that is transmitted by the q^{th} BS at time t during the k^{th} time slot, $S_{q,k}[f] \triangleq \frac{1}{\sqrt{2\pi}} \int_{-\infty}^{\infty} s_{q,k}[t] \exp\left(-j2\pi f t\right) \ dt$. The properties of the received signals are

1) Effective Baseband Bandwidth: This relates to the variance of all the occupied frequencies. From the system definition, we have two effective baseband bandwidths $\alpha_{1b,k} \triangleq$

$$\left(\frac{\int_{-\infty}^{\infty} f^2 |S_{b,k}[f]|^2 df}{\int_{-\infty}^{\infty} |S_{b,k}[f]|^2 df}\right)^{\frac{1}{2}}, \text{ and } \alpha_{1q,k} \triangleq \left(\frac{\int_{-\infty}^{\infty} f^2 |S_{q,k}[f]|^2 df}{\int_{-\infty}^{\infty} |S_{q,k}[f]|^2 df}\right)^{\frac{1}{2}}.$$

helps to provide a compact representation of the mathematical description of the available information in the received signals. $\alpha_{2b,k} \triangleq \frac{\int_{-\infty}^{\infty} f|S_{b,k}[f]|^2 df}{\left(\int_{-\infty}^{\infty} f^2|S_{b,k}[f]|^2 df\right)^{\frac{1}{2}}\left(\int_{-\infty}^{\infty} f|S_{b,k}[f]|^2 df\right)^{\frac{1}{2}}\left(\int_{-\infty}^{\infty} |S_{b,k}[f]|^2 df\right)^{\frac{1}{2}}}$, and $\alpha_{2q,k} \triangleq \frac{\int_{-\infty}^{\infty} f|S_{q,k}[f]|^2 df}{\left(\int_{-\infty}^{\infty} f^2|S_{q,k}[f]|^2 df\right)^{\frac{1}{2}}\left(\int_{-\infty}^{\infty} |S_{q,k}[f]|^2 df\right)^{\frac{1}{2}}}$.

3) Received Signal-to-Noise Ratio: The SNR quantifies the

ratio of the power of the signal across its occupied frequencies to the noise spectral density. Mathematically, given the system model, the SNRs are

III. AVAILABLE INFORMATION ABOUT CHANNEL PARAMETERS IN THE RECEIVED SIGNAL

The information about the channel parameters in the received signal is presented in this section and serves as an intermediate step to investigate the information needed for localization.

A. Geometric and nuisance channel parameters

We can represent the observable parameters in signals from the N_B LEOs across the N_U antennas during the N_K time slots in vector form as: $\boldsymbol{\eta}_{bU} \triangleq \left[\boldsymbol{\tau}_{bU}^{\mathrm{T}}, \boldsymbol{\nu}_{bU}^{\mathrm{T}}, \beta_{bU}, \delta_{bU}, \epsilon_{bU}\right]^{\mathrm{T}}$. We can represent the observable parameters in signals from the N_Q BSs across the N_U antennas during the N_K time slots in vector form as: $\boldsymbol{\eta}_{qU} \triangleq \left[\boldsymbol{\tau}_{qU}^{\mathrm{T}}, \boldsymbol{\nu}_{qU}^{\mathrm{T}}, \beta_{qU}, \delta_{QU}, \epsilon_{QU}\right]^{\mathrm{T}}$. Lastly, we focus on parameters in the LEOs-BSs links. We can represent the observable parameters in signals from the N_B LEOs at all the N_Q BSs during the N_K time slots in vector form as: $\boldsymbol{\eta}_{bQ} \triangleq \left[\boldsymbol{\tau}_{bQ}^{\mathrm{T}}, \boldsymbol{\nu}_{bQ}^{\mathrm{T}}, \boldsymbol{\beta}_{bQ}^{\mathrm{T}}, \delta_{bQ}, \epsilon_{bQ}\right]^{\mathrm{T}}$. We have specified all the parameters that are observable in

the received signals. In the next section, we present mathematical preliminaries that help determine the information available about these parameters in the received signals.

B. Mathematical Preliminaries

In estimation theory, two questions of paramount importance are the parameters that can be estimated and the conditions that allow for the estimation of these parameters. One way of answering these questions is through the Fisher information matrix (FIM). To present the FIM, we assume that for the parameters and system model in our work, there exists an unbiased estimate $\hat{\boldsymbol{\eta}}$ such that the error covariance matrix satisfies the following information inequality $\mathbb{E}_{\boldsymbol{y};\boldsymbol{\eta}}\left\{(\hat{\boldsymbol{\eta}}-\boldsymbol{\eta})(\hat{\boldsymbol{\eta}}-\boldsymbol{\eta})^{\mathrm{T}}\right\}\succeq\mathbf{J}_{\boldsymbol{y};\boldsymbol{\eta}}^{-1},$ where $\mathbf{J}_{\boldsymbol{y};\boldsymbol{\eta}}$ is the FIM for the parameter vector $\boldsymbol{\eta}.$

Definition 1. The FIM obtained from the likelihood due to the observations is defined as $\mathbf{J}_{y;\eta} = \mathbf{F}_y(y|\eta;\eta,\eta)$. In mathematical terms, we have

$$\mathbf{J}_{\boldsymbol{y};\boldsymbol{\eta}} \triangleq -\mathbb{E}_{\boldsymbol{y};\boldsymbol{\eta}} \left[\frac{\partial^2 \ln \chi(\boldsymbol{y};\boldsymbol{\eta})}{\partial \boldsymbol{\eta} \partial \boldsymbol{\eta}^{\mathrm{T}}} \right] \tag{7}$$

where $\chi(y; \eta)$ denotes the likelihood function considering y and η .

The FIM is a very useful tool, however it grows quadratically with the size of the parameter vector. Hence, it might be advantageous to focus on a subset of the FIM. One way to do this is to use the equivalent FIM (EFIM) [11].

Definition 2. Given a parameter vector, $\boldsymbol{\eta} \triangleq \begin{bmatrix} \boldsymbol{\eta}_1^{\mathrm{T}}, \boldsymbol{\eta}_2^{\mathrm{T}} \end{bmatrix}^{\mathrm{T}}$, where $\boldsymbol{\eta}_1$ is the parameter of interest, the resultant FIM has the structure

$$\mathbf{J}_{\boldsymbol{y};\boldsymbol{\eta}} = \left[\begin{array}{ccc} \mathbf{J}_{\boldsymbol{y};\eta_1} & \mathbf{J}_{\boldsymbol{y};\eta_1,\eta_2} \\ \mathbf{J}_{\boldsymbol{y};\eta_1,\eta_2}^{\mathrm{T}} & \mathbf{J}_{\boldsymbol{y};\eta_2} \end{array} \right],$$

where $\eta \in \mathbb{R}^N, \eta_1 \in \mathbb{R}^n, \mathbf{J}_{\boldsymbol{y};\eta_1} \in \mathbb{R}^{n \times n}, \mathbf{J}_{\boldsymbol{y};\eta_1,\eta_2} \in \mathbb{R}^{n \times (N-n)}, \text{ and } \mathbf{J}_{\boldsymbol{y};\eta_2} \in \mathbb{R}^{(N-n) \times (N-n)} \text{ with } n < N, \text{ and } the EFIM [12] of parameter <math>\eta_1$ is given by $\mathbf{J}_{\boldsymbol{y};\eta_1}^{\mathrm{e}} = \mathbf{J}_{\boldsymbol{y};\eta_1} - \mathbf{J}_{\boldsymbol{y};\eta_1}^{nu} = \mathbf{J}_{\boldsymbol{y};\eta_1} - \mathbf{J}_{\boldsymbol{y};\eta_1,\eta_2}^{nu} \mathbf{J}_{\boldsymbol{y};\eta_1}^{-1} \mathbf{J}_{\boldsymbol{y};\eta_1,\eta_2}^{\mathrm{T}}.$

 $\mathbf{J}_{\boldsymbol{y};\boldsymbol{\eta}_1}^{nu} = \mathbf{J}_{\boldsymbol{y};\boldsymbol{\eta}_1} - \mathbf{J}_{\boldsymbol{y};\boldsymbol{\eta}_1,\boldsymbol{\eta}_2} \mathbf{J}_{\boldsymbol{y};\boldsymbol{\eta}_1}^{-1} \mathbf{J}_{\boldsymbol{y};\boldsymbol{\eta}_1,\boldsymbol{\eta}_2}^{\mathrm{T}}.$ Note that the term $\mathbf{J}_{\boldsymbol{y};\boldsymbol{\eta}_1}^{nu} = \mathbf{J}_{\boldsymbol{y};\boldsymbol{\eta}_1,\boldsymbol{\eta}_2} \mathbf{J}_{\boldsymbol{y};\boldsymbol{\eta}_2}^{\mathrm{T}} \mathbf{J}_{\boldsymbol{y};\boldsymbol{\eta}_1,\boldsymbol{\eta}_2}^{\mathrm{T}}$ describes the loss of information about $\boldsymbol{\eta}_1$ due to uncertainty in the nuisance parameters $\boldsymbol{\eta}_2$. This EFIM captures all the required information about the parameters of interest present in the FIM; as observed from the relation $(\mathbf{J}_{\boldsymbol{y};\boldsymbol{\eta}_1}^{\mathrm{e}})^{-1} = [\mathbf{J}_{\boldsymbol{y};\boldsymbol{\eta}}^{-1}]_{[1:n,1:n]}$.

C. FIM for channel parameters

To derive the FIM for the channel parameters, we note that likelihood is given by (8) in [2]. Considering all the N_B LEOs, N_K transmission time slots, and N_U receive antennas, we can derive the FIMs for both cases of parameterization. The FIMs for both parameterization cases result in a block diagonal. The first case of parameterization produces

$$\mathbf{J}_{\boldsymbol{y}|\boldsymbol{\eta}} = \boldsymbol{F}_{\boldsymbol{y}}(\boldsymbol{y}|\boldsymbol{\eta};\boldsymbol{\eta},\boldsymbol{\eta}) = \\
\operatorname{diag} \left\{ \boldsymbol{F}_{\boldsymbol{y}}(\boldsymbol{y}|\boldsymbol{\eta};\boldsymbol{\eta}_{1U},\boldsymbol{\eta}_{1U}), \dots, \boldsymbol{F}_{\boldsymbol{y}}(\boldsymbol{y}|\boldsymbol{\eta};\boldsymbol{\eta}_{N_BU},\boldsymbol{\eta}_{N_BU}) \right. \\
\left. \boldsymbol{F}_{\boldsymbol{y}}(\boldsymbol{y}|\boldsymbol{\eta};\boldsymbol{\eta}_{1U},\boldsymbol{\eta}_{1U}), \dots, \boldsymbol{F}_{\boldsymbol{y}}(\boldsymbol{y}|\boldsymbol{\eta};\boldsymbol{\eta}_{N_QU},\boldsymbol{\eta}_{N_QU}) \right. \\
\left. \boldsymbol{F}_{\boldsymbol{y}}(\boldsymbol{y}|\boldsymbol{\eta};\boldsymbol{\eta}_{1Q},\boldsymbol{\eta}_{1Q}), \dots, \boldsymbol{F}_{\boldsymbol{y}}(\boldsymbol{y}|\boldsymbol{\eta};\boldsymbol{\eta}_{N_BQ},\boldsymbol{\eta}_{N_BQ}) \right\}.$$
(8)

Considering the LEOs-receiver link, the entries in FIM due to the observations of the signals at the receiver from $b^{\rm th}$ LEO satellite can be obtained through the simplified expression.

$$\begin{aligned} \boldsymbol{F_y}(\boldsymbol{y}|\boldsymbol{\eta};\boldsymbol{\eta}_{bU},\boldsymbol{\eta}_{bU}) &= \frac{1}{N_{01}} \times \\ &\sum_{u,k}^{N_U N_K} \Re \left\{ \int \nabla_{\boldsymbol{\eta}_{bU}} \mu_{bu,k}[t] \nabla_{\boldsymbol{\eta}_{bU}} \mu_{bu,k}^{\mathrm{H}}[t] \ dt \right\} \end{aligned}$$

We now present the non-zero entries focusing on the $b^{\rm th}$ LEO satellite. We start with the delays focusing on the FIM for the delay from the $b^{\rm th}$ LEO satellite during the $k^{\rm th}$ time slot on the $u^{\rm th}$ receive antenna.

$$F_{\boldsymbol{y}}(\boldsymbol{y}|\boldsymbol{\eta}; \tau_{bu,k}, \tau_{bu,k}) = -F_{\boldsymbol{y}}(\boldsymbol{y}|\boldsymbol{\eta}; \tau_{bu,k}, \delta_{bU}) = \underset{bu,k}{\text{SNR}} \omega_{bU,k},$$

where
$$\omega_{bU,k} = \left[\alpha_{1b,k}^2 + 2f_{obU,k}\alpha_{1b,k}\alpha_{2b,k} + f_{obU,k}^2\right]$$
. All other entries in the FIM focusing on delays in the b^{th} LEO link are zero. The FIM focusing on the Dopplers related to the b^{th} LEO satellite is $F_y(y|\eta;\nu_{bU,k},\nu_{bU,k}) = 0.5* \mathrm{SNR}\,f_c^2t_{obu,k}^2$. The FIM of the Doppler observed with respect to the b^{th} LEO satellite and the corresponding frequency offset during the k^{th} time slot is $F_y(y|\eta;\nu_{bU,k},\epsilon_{bU}) = -0.5* \mathrm{SNR}\,f_ct_{obu,k}^2$. All other entries in the FIM related to the Dopplers in the b^{th} LEO link are zero. Now, we focus on the channel gain in the b^{th} LEO link. The FIM of the channel gain considering the received signals from b^{th} LEO satellite to the u^{th} receive antenna during the k^{th} time slot is $F_y(y|\eta;\beta_{bu,k},\beta_{bu,k}) = \frac{1}{4\pi^2\,|\beta_{bu,k}|^2} \frac{\mathrm{SNR}}{bu,k}$. All other entries in the FIM related to the channel gain in the b^{th} LEO link are zero. Now, we focus on the time offset in the b^{th} LEO link. The FIM between the time offset and the delay in the FIM due to the observations of the received signals from b^{th} LEO satellite to the u^{th} receive antenna during the k^{th} time slot is $F_y(y|\eta;\delta_{bU},\tau_{bu,k}) = F_y(y|\eta;\tau_{bu,k},\delta_{bU})$. The FIM of the time offset in the FIM due to the observations of the received signals from b^{th} LEO satellite to the u^{th} receive antenna during the k^{th} time slot is FIM due to the observations of the received signals from b^{th} LEO satellite to the u^{th} receive antenna during the k^{th} time slot is

$$F_{\mathbf{y}}(\mathbf{y}|\boldsymbol{\eta};\delta_{bU},\delta_{bU}) = F_{\mathbf{y}}(\mathbf{y}|\boldsymbol{\eta};\tau_{bu,k},\tau_{bu,k}) = -F_{\mathbf{y}}(\mathbf{y}|\boldsymbol{\eta};\delta_{bU},\tau_{bu,k}).$$

All other entries in the FIM related to the time offset in the $b^{\rm th}$ LEO link are zero. The FIMs related to the frequency offset are presented next. The FIM of the frequency offset and the corresponding Doppler observed with respect to the $b^{\rm th}$ LEO satellite during the $k^{\rm th}$ time slot is $F_{\boldsymbol{y}}(\boldsymbol{y}|\boldsymbol{\eta};\epsilon_{bU},\nu_{b,k}) = -0.5* \underset{bu,k}{\rm SNR} f_c t_{obu,k}^2$. The FIM of the frequency offset in the FIM due to the observations of the received signals from $b^{\rm th}$ LEO satellite to the $u^{\rm th}$ receive antenna during the $k^{\rm th}$ time slot is $F_{\boldsymbol{y}}(\boldsymbol{y}|\boldsymbol{\eta};\epsilon_{bU},\epsilon_{bU}) = 0.5* \underset{bu,k}{\rm SNR} t_{obu,k}^2$.

The FIM for the channel parameters in the BSs-receiver and LEO-BSs links are presented in [2].

IV. FIM FOR LOCATION PARAMETERS

In the previous sections, we have presented a system model that captures unsynchronized LEOs in time and frequency communicating with a receiver and a set of synchronized BSs. We also presented a system model incorporating the BSs communicating with the receiver. Subsequently, we derived the available information in the received signals using the FIM. In this section, we first highlight the location parameters and transform the FIM for the channel parameters into the FIM for location parameters. To highlight the location parameters, we i) focus on the unknown receiver position at k=0, $p_{U,0}$, ii) assume that the receiver velocity remains constant

across all N_K time slots, $\boldsymbol{v}_{U,k} = \boldsymbol{v}_{U,0} \quad \forall k$, iii) assume that the uncertainty associated with the position of the b^{th} LEO remains constant across all N_K time slots $\check{\boldsymbol{p}}_{b,k} = \check{\boldsymbol{p}}_{b,0} \quad \forall k$, and iv) assume that the uncertainty associated with the velocity of the b^{th} LEO remains constant across all N_K time slots $\check{\boldsymbol{v}}_{b,k} = \check{\boldsymbol{v}}_{b,0} \quad \forall k$. Now, we highlight the location parameters as

$$\kappa =$$

 $egin{aligned} [oldsymbol{p}_{U,0},oldsymbol{v}_{U,0},oldsymbol{\Phi}_{U},oldsymbol{p}_{B,0},oldsymbol{v}_{B,0},oldsymbol{\zeta}_{1U},\cdots,oldsymbol{\zeta}_{N_{B}U},oldsymbol{\zeta}_{1Q},\cdots,oldsymbol{\zeta}_{N_{B}Q},\ oldsymbol{\zeta}_{1U},\cdots,oldsymbol{\zeta}_{N_{Q}U}], \end{aligned}$

where

$$\begin{split} \check{\boldsymbol{p}}_{B,0} &= \left[\check{\boldsymbol{p}}_{1,0}^{\mathrm{T}}, \cdots, \check{\boldsymbol{p}}_{N_{B},0}^{\mathrm{T}}\right]^{\mathrm{T}}, \check{\boldsymbol{v}}_{B,0} &= \left[\check{\boldsymbol{v}}_{1,0}^{\mathrm{T}}, \cdots, \check{\boldsymbol{v}}_{N_{B},0}^{\mathrm{T}}\right]^{\mathrm{T}}, \\ \boldsymbol{\zeta}_{bU} &= \left[\boldsymbol{\beta}_{bU}^{\mathrm{T}}, \delta_{bU}, \epsilon_{bU}\right]^{\mathrm{T}}, \boldsymbol{\zeta}_{bQ} &= \left[\boldsymbol{\beta}_{bQ}^{\mathrm{T}}, \delta_{bQ}, \epsilon_{bQ}\right]^{\mathrm{T}}, \\ \boldsymbol{\zeta}_{aU} &= \left[\boldsymbol{\beta}_{aU}^{\mathrm{T}}, \delta_{QU}, \epsilon_{QU}\right]^{\mathrm{T}}. \end{split}$$

The location parameter vector, κ , can be divided into $\kappa_1 = [p_{U,0}, v_{U,0}, \Phi_U, \check{p}_{b,0}, \check{v}_{b,0}]$ and $\kappa_2 = [\zeta_{1U}, \cdots, \zeta_{N_BU}, \zeta_{1Q}, \cdots, \zeta_{N_BQ}, \zeta_{1U}, \cdots, \zeta_{N_QU}]$. The FIM for the location parameters can be obtained from the FIM for the channel parameters $\mathbf{J}_{y|\eta}$, using the bijective transformation $\mathbf{J}_{y|\kappa} \triangleq \Upsilon_{\kappa} \mathbf{J}_{y|\eta} \Upsilon_{\kappa}^{\mathrm{T}}$, where Υ_{κ} represents derivatives of the non-linear relationship between the geometric channel parameters, η , and the location parameters [13]. The elements in the bijective transformation matrix Υ_{κ} are given in Appendix A. The EFIM taking $\kappa_1 = [p_{U,0}, v_{U,0}, \Phi_U, \check{p}_{b,0}, \check{v}_{b,0}]$ as the parameter of interest and $\kappa_2 = [\zeta_{1U}, \cdots, \zeta_{N_BU}, \zeta_{1Q}, \cdots, \zeta_{N_BQ}, \zeta_{1U}, \cdots, \zeta_{NQU}]$ as the nuisance parameters is now derived.

A. FIM for the parameters of interest

Here, we present the FIM for the parameters of interest, κ_1 . This FIM is represented by $\mathbf{J}_{y|\kappa_1}$, and the entries in this FIM are presented in the following Lemmas.

Lemma 1. The FIM of the 3D position of the receiver is

$$F_{y}(\boldsymbol{y}|\boldsymbol{\eta};\boldsymbol{p}_{U,0},\boldsymbol{p}_{U,0}) = \text{combinations of } N_{B}, N_{K}, N_{Q}, \text{ and } N_{U} \text{ that produce a positive}$$

$$\sum_{b,k,u} \frac{\text{SNR}}{c^{2}} \frac{\omega_{bU,k}}{c^{2}} \boldsymbol{\Delta}_{bu,k} \boldsymbol{\Delta}_{bu,k}^{\mathrm{T}} + \frac{f_{c}^{2} t_{obu,k}^{2} \nabla_{\boldsymbol{p}_{U,0}} \nu_{bU,k} \nabla_{\boldsymbol{p}_{U,0}}^{\mathrm{T}} \nu_{bU,k}}{2} \text{ definite } \mathbf{J}_{\boldsymbol{y}|\kappa_{1}}^{\mathbf{e}}. \text{ It is important to note that while [1] indicates}$$

$$\sum_{q,k,u} \frac{\text{SNR}}{c^{2}} \frac{\omega_{qU,k}}{c^{2}} \boldsymbol{\Delta}_{qu,k} \boldsymbol{\Delta}_{qu,k}^{\mathrm{T}} + \frac{f_{c}^{2} t_{oqu,k}^{2} \nabla_{\boldsymbol{p}_{U,0}} \nu_{qU,k} \nabla_{\boldsymbol{p}_{U,0}}^{\mathrm{T}} \nu_{qU,k}}{2} \text{ of uncertainty in the LEO ephemeris changes the analysis}$$

$$\sum_{q,k,u} \frac{\omega_{qU,k}}{c^{2}} \boldsymbol{\Delta}_{qu,k} \boldsymbol{\Delta}_{qu,k}^{\mathrm{T}} + \frac{f_{c}^{2} t_{oqu,k}^{2} \nabla_{\boldsymbol{p}_{U,0}} \nu_{qU,k} \nabla_{\boldsymbol{p}_{U,0}}^{\mathrm{T}} \nu_{qU,k}}{2} \text{ of uncertainty in the LEO ephemeris changes the analysis}$$
and results. Moreover, the presence of signals from 5G base stations adds another dimension. Hence, in this section, we

Lemma 2. The FIM of the 3D velocity of the receiver is

$$F_{y}(y|\eta; v_{U,0}, v_{U,0}) = \sum_{b,k,u} \frac{SNR}{su,k} \left[\frac{(k-1)^{2} \omega_{bU,k} \Delta_{t}^{2}}{c^{2}} \Delta_{bu,k} \Delta_{bu,k}^{T} + \frac{f_{c}^{2} t_{obu,k}^{2} \Delta_{bU,k} \Delta_{bU,k}^{T}}{2 c^{2}} \right] + \sum_{q,k,u} \frac{SNR}{qu,k} \left[\frac{(k-1)^{2} \omega_{qU,k} \Delta_{t}^{2}}{c^{2}} \Delta_{qu,k} \Delta_{qu,k}^{T} + \frac{f_{c}^{2} t_{oqu,k}^{2} \Delta_{qU,k} \Delta_{qU,k}^{T}}{2 c^{2}} \right].$$
(10)

Lemma 3. The FIM for the 3D orientation of the receiver is

$$F_{y}(y|\eta; \mathbf{\Phi}_{U}, \mathbf{\Phi}_{U}) = \sum_{b,k,u} \operatorname{SNR}_{bu,k} \left[\omega_{bU,k} \nabla_{\mathbf{\Phi}_{U}} \tau_{bu,k} \nabla_{\mathbf{\Phi}_{U}}^{\mathrm{T}} \tau_{bu,k} \right] + \sum_{q,k,u} \operatorname{SNR}_{qu,k} \left[\omega_{qU,k} \nabla_{\mathbf{\Phi}_{U}} \tau_{qu,k} \nabla_{\mathbf{\Phi}_{U}}^{\mathrm{T}} \tau_{qu,k} \right].$$

$$(11)$$

Lemma 4. The FIM for the 3D position uncertainty associated with the b^{th} LEO, $\check{p}_{b,0}$ is

$$F_{y}(\boldsymbol{y}|\boldsymbol{\eta}; \boldsymbol{\check{p}}_{b,0}, \boldsymbol{\check{p}}_{b,0}) = \sum_{k,u} \frac{SNR}{bu,k} \left[\frac{\omega_{bU,k}}{c^{2}} \boldsymbol{\Delta}_{bu,k} \boldsymbol{\Delta}_{bu,k}^{T} + \frac{f_{c}^{2} t_{obu,k}^{2} \nabla_{\boldsymbol{\check{p}}_{b,0}} \nu_{bU,k} \nabla_{\boldsymbol{\check{p}}_{b,0}}^{T} \nu_{bU,k}}{2} \right] + \sum_{q,k} \frac{SNR}{bq,k} \left[\frac{\omega_{bq,k}}{c^{2}} \boldsymbol{\Delta}_{bq,k} \boldsymbol{\Delta}_{bq,k}^{T} + \frac{f_{c}^{2} t_{obq,k}^{2} \nabla_{\boldsymbol{\check{p}}_{b,0}} \nu_{bq,k} \nabla_{\boldsymbol{\check{p}}_{b,0}}^{T} \nu_{bq,k}}{2} \right].$$

$$(12)$$

Lemma 5. The FIM for the 3D velocity uncertainty associated with the b^{th} LEO, $\check{v}_{b,0}$ is

$$F_{y}(\boldsymbol{y}|\boldsymbol{\eta}; \boldsymbol{\check{v}}_{b,0}, \boldsymbol{\check{v}}_{b,0}) =$$

$$\sum_{k,u} \underset{bu,k}{\text{SNR}} \left[\frac{(k-1)^{2} \omega_{bU,k} \Delta_{t}^{2}}{c^{2}} \boldsymbol{\Delta}_{bu,k} \boldsymbol{\Delta}_{bu,k}^{\text{T}} + \frac{f_{c}^{2} t_{obu,k}^{2} \boldsymbol{\Delta}_{bU,k} \boldsymbol{\Delta}_{bU,k}^{\text{T}}}{2 c^{2}} \right] +$$

$$\sum_{q,k} \underset{bq,k}{\text{SNR}} \left[\frac{(k-1)^{2} \omega_{bq,k} \Delta_{t}^{2}}{c^{2}} \boldsymbol{\Delta}_{bq,k} \boldsymbol{\Delta}_{bq,k}^{\text{T}} + \frac{f_{c}^{2} t_{obq,k}^{2} \boldsymbol{\Delta}_{bq,k} \boldsymbol{\Delta}_{bq,k}^{\text{T}}}{2 c^{2}} \right].$$

$$(13)$$

Proof. For proof of these lemmas, see Appendix B. \Box

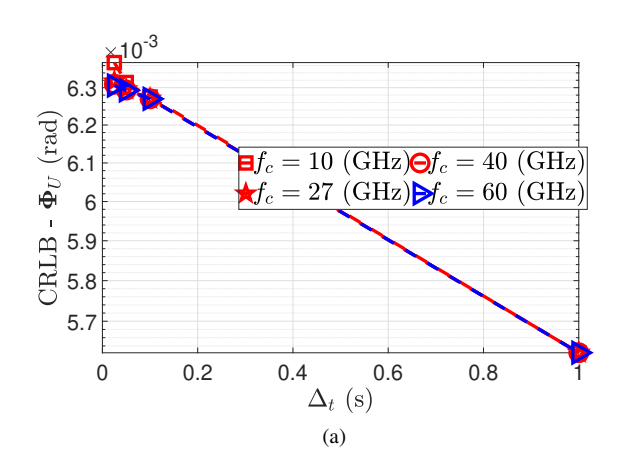
B. Loss in information due to uncertainty about the parameters of interest

The reduction in information about the parameter of interest due to the nuisance parameters is presented in Section IV-B in [2].

V. NUMERICAL RESULTS

In this section, we use simulations to determine the minimal combinations of N_B , N_K , N_Q , and N_U that produce a positive definite $\mathbf{J}_{y|\kappa_1}^{\mathrm{e}}$. It is important to note that while [1] indicates that using 3 LEO satellites, 3 time slots, and $N_U>1$ is enables the 9D localization of a receiver, the presence of uncertainty in the LEO ephemeris changes the analysis and results. Moreover, the presence of signals from 5G base stations adds another dimension. Hence, in this section, we investigate the use of signals in the LEO-receiver, LEO-BS, and BS-receiver links for both 9D localization and ephemeris correction. This investigation is carried out by analyzing the conditions that make $\mathbf{J}_{y|\kappa_1}^{\mathrm{e}}$ positive definite. We notice that $\mathbf{J}_{y|\kappa_1}^{\mathrm{e}}$ is positive definite when $N_B=1$, if $N_K>=3$, $N_U>1$, and $N_Q>=3$. Again, the matrix $\mathbf{J}_{y|\kappa_1}^{\mathrm{e}}$ is positive definite when $N_B=2$, if $N_K>=3$, $N_U>1$, and $N_Q>=3$. Finally, the matrix $\mathbf{J}_{y|\kappa_1}^{\mathrm{e}}$ is positive definite when $N_B=3$, if $N_K>=4$, $N_U>1$, and $N_Q>=3$. These conditions for joint 9D localization and ephemeris correction are obtained using

the following simulation parameters. The following frequencies are considered $f_c \in [10, 27, 40, 60]$ GHz. The following spacings between transmission time slots are considered $\Delta_t \in$ [25, 50, 100, 1000, 10000, 20000, 50000] ms. We consider the following number of LEOs and BSs $N_B \in [1,2,3]$ and $N_Q \in [1,2,3,4]$, respectively. The 3D coordinates of the LEOs are randomly chosen, but the LEOs are approximately 2000 km from the receiver. The 3D coordinates of the receiver and the BSs are also randomly chosen, but their distances are 30 m and 100 m from the origin, respectively. The BSs are stationary. However, the 3D velocity of the LEOs and receiver are randomly chosen, but their speeds are 8000 m/s and 25 m/s, respectively. The velocity of the LEOs is modeled to change every time slot to capture the acceleration of the LEOs. However, the velocity of the receiver remains constant across all transmission time slots. For all links, the effective baseband bandwidth is 100 MHz, and the BCC is 0 MHz. For the b^{th} LEO and q^{th} BS, we assume that the same signal is transmitted across all N_K time slots, and the channel gain is constant across all receive antennas and time slots. The CRLBs for $\mathbf{p}_{U,0}$, $\mathbf{v}_{U,0}$, $\mathbf{\Phi}_{U}$, $\check{\mathbf{p}}_{b,0}$, and $\check{\mathbf{v}}_{b,0}$ are obtained by inverting $\mathbf{J}_{y|\kappa_1}^{\mathrm{e}}$ and summing the appropriate diagonals. In Fig. 2a, we notice that the CRLB of Φ_U is not impacted by the center frequency. From 2b, we notice that the number of receive antennas does not substantially impact the CRLB obtainable during estimation of $\check{\mathbf{v}}_{b,0}$.



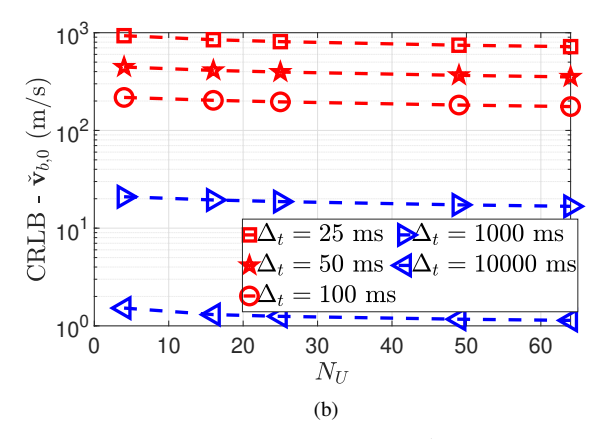


Figure 2. (a) CRLB of Φ_U as a function of Δ_t . (b) CRLB of $\check{\mathbf{v}}_{b,0}$ as a function of N_U . For both plots, $N_U=64$, the SNR is 20 dB which is constant across all links, $N_Q=3$, $N_B=3$ and $N_K=4$.

VI. CONCLUSION

This paper has explored utilizing LEOs and 5G BSs for both 9D receiver localization and LEO ephemeris correction. We showed through the FIM that i) with one LEO, we need three BSs and three-time slots to both estimate the 9D location parameters and correct the LEO position and velocity, ii) with two LEO, we need three BSs and three-time slots to both estimate the 9D location parameters and correct the LEO position and velocity, and iii) with three LEO, we need three BSs and four-time slots to both estimate the 9D location parameters and correct the LEO position and velocity. We noticed from the CRLB that the operating frequency and number of receive antennas have negligible impact on the estimation accuracy of the orientation of the receiver and the LEO velocity, respectively.

APPENDIX

A. Entries in transformation matrix
See Appendix A in [2].

B. Proof of elements in $J_{y;\kappa_1}$ See Appendix B in [2].

REFERENCES

- D.-R. Emenonye, H. S. Dhillon, and R. M. Buehrer, "Fundamentals of LEO based localization," in preparation for IEEE Trans. on Info. Theory, 2024.
- [2] —, "Joint 9D receiver localization and ephemeris correction with LEO and 5G base stations," in preparation for IEEE Trans. on Info. Theory, 2024.
- [3] J. Kang, P. E. N, J. Lee, H. Wymeersch, and S. Kim, "Fundamental performance bounds for carrier phase positioning in LEO-PNT systems," in *Proc.*, *IEEE Intl. Conf. on Acoustics, Speech, and Sig. Proc. (ICASSP)*, 2024, pp. 13496–13500.
- [4] T. Reid, A. Neish, T. Walter, and P. Enge, "Broadband LEO constellations for navigation," *Navigation*, vol. 65, Jun. 2018.
- [5] A. Nardin, F. Dovis, and J. A. Fraire, "Empowering the tracking performance of LEO-based positioning by means of meta-signals," *IEEE J. of Radio Frequency Identification*, vol. 5, no. 3, pp. 244–253, Sep. 2021.
- [6] L. You, X. Qiang, Y. Zhu, F. Jiang, C. G. Tsinos, W. Wang, H. Wymeer-sch, X. Gao, and B. Ottersten, "Integrated communications and localization for massive MIMO LEO satellite systems," *IEEE Trans. on Wireless Commun.*, to appear.
- [7] M. L. Psiaki, "Navigation using carrier doppler shift from a LEO constellation: TRANSIT on steroids," NAVIGATION, vol. 68, no. 3, pp. 621–641, 2021. [Online]. Available: https://onlinelibrary.wiley.com/doi/abs/10.1002/navi.438
- [8] Z. M. Kassas, J. Morales, and J. J. Khalife, "New-age satellite-based navigation – STAN: Simultaneous tracking and navigation with LEO satellite signals," 2019. [Online]. Available: https://api.semanticscholar.org/CorpusID:214300844
- [9] J. Khalife, M. Neinavaie, and Z. M. Kassas, "Navigation with differential carrier phase measurements from megaconstellation LEO satellites," in *Proc.*, *IEEE/ION Position, Location and Navigation Symposium* (*PLANS*), 2020, pp. 1393–1404.
- [10] S. M. LaValle, Planning Algorithms. Cambridge University Press, 2006.
- [11] R. A. Horn and C. R. Johnson, *Matrix Analysis*. Cambridge University Press, 2012.
- [12] Y. Shen and M. Z. Win, "Fundamental limits of wideband localization—part I: A general framework," *IEEE Trans. on Info. Theory*, vol. 56, no. 10, pp. 4956–4980, Oct. 2010.
- [13] S. M. Kay, Fundamentals of Statistical Signal Processing: Estimation Theory. Prentice-Hall, Inc., 1993.